Design Of Basic Double Gauss Lenses

Mandler, Walter

Walter Mandler, "Design Of Basic Double Gauss Lenses," Proc. SPIE 0237, 1980 International Lens Design Conference, (16 September 1980); doi: 10.1117/12.959089

Event: 1980 International Lens Design Conference, 1980, Oakland, United States

Design of basic double Gauss lenses

Walter Mandler
P.O. Box 453, Midland, Ontario, Canada, L4R 4L3
(The work has been sponsored by Ernst Leitz Wetzlar GmbH)

Abstract

A procedure for the design of basic Double Gauss lenses has been developed that uses fifth-order interpolating aberrations in the framework of a damped-least-squares program. It proceeds from a rough model directly to a solution.

Introduction

The Double Gauss lens and its variations constitute a major percentage of all photographic lenses currently in production. However, literature on the synthesis of these lenses is very scarce. In patents and textbook articles, many isolated statements with regard to the relationship between selected aberrations and parameters are given, but I have not been able to find a formalized procedure for the synthesis of Double Gauss lenses. Matsui and Hirose[1] describe an approach to the problem which remains incomplete because the determination of the starting data for the inner menisci is not given, and repeated adjustments of the target values are required in order to obtain a well corrected lens.

In the following, a design procedure for basic Double Gauss lenses will be demonstrated that provides the starting configurations for a DLS optimization program and leads directly to a well corrected lens.

The basic Double Gauss lens consists of two outer lenses and two inner cemented menisci, symmetrically arranged with regard to the diaphragm. In a previous paper by this author[2], the special case of equal refractive index for the main wavelength of the two elements of the cemented menisci has been treated. (That is, both menisci are hyperchromatic lenses, as used by Rudolph in the first Planar lens[3].) This presentation reports the main results of [2] and extends to the case of index differences at the cemented surfaces of the menisci.

Calculation of Starting Data

Disregarding the cemented surfaces in the menisci, a very rough approximation of the basic Double Gauss lens may be conceived as a variation of the triplet. The centre lens is seen to be replaced by 2 equal concentric menisci, arranged symmetrically with regard to the diaphragm and the outer lenses are seen as equal plano-convex lenses arranged likewise. See Figure 1.

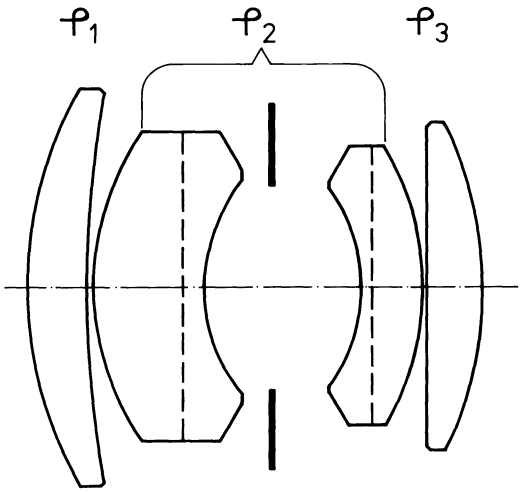

Figure 1. Triplet Model

With total power Φ, component powers ϕ_1, ϕ_2, ϕ_3 and spaces t_1 and t_2 we have for a triplet in general

$$(1) \quad \Phi = \phi_1 + \phi_2 + \phi_3 = t_1\phi_1(\phi_2 + \phi_3) - t_2\phi_3(\phi_1 + \phi_2) + t_1t_2\phi_1\phi_2\phi_3$$

For thick lenses t_1 and t_2 are the distances between the appropriate principal points. If the arrangement is symmetrical to the stop, we obtain $\phi_1 = \phi_3$; $t_1 = t_2$. We stipulate $\phi_2 = -\phi_1$ and obtain

$$(2a) \quad \Phi = \phi_1 - t_1^2\phi_1^3 \qquad 2(b) \quad f = \frac{f_1^3}{f_1^2 - t_1^2}$$

From (2b) we can calculate f_1 if f and t_1 are given. In the following for all calculations, we will assume f=52 and $t_1 \simeq 16$; that is, we are looking at the most common standard focal length for the 35 mm format and maintain an approximate overall length of 36 mm.

For a given refractive index n the radii of the first and last (plano-convex) lenses are $r_1 = f_1(n-1)$. The relationship between focal length and construction data for the combination of 2 concentric menisci does not lead itself to a simple explicit expression for one of the meniscus radii. Therefore, they are to be determined by successive approximations for a meniscus thickness of 7 mm and a distance to the stop of 6 mm to obtain a table of data for different refractive indices.

Table 1. Starting Data

Surface No.		1 (9)	2 (8)	3 (7)	4 (6)	5
Thickness (Space)		4.0	0.2	7.0	6.0	
n = 1.57	Radius	26.02	∞	18.61	11.61	Stop
n = 1.62	Radius	28.30	∞	18.99	11.99	Stop
n = 1.66	Radius	30.13	∞	19.27	12.27	Stop
n = 1.69	Radius	31.50	∞	19.47	12.47	Stop
n = 1.75	Radius	33.78	∞	19.79	12.79	Stop
n = 1.79	Radius	36.06	∞	20.08	13.08	Stop

The rear half of the system is symmetrical. Therefore, radii 6 through 9 have the opposite signs of radii 1 through 4.

Table 1 gives us starting data for six lenses. Later we will generate starting data for lenses consisting of elements with different refractive indices by taking the appropriate data from different lines of Table 1. The refractive indices in Table 1 have been selected because they correspond to popular glasses. The ascending indices for crown glasses have become available in the years indicated.

Table 2.

Refractive Index	1.57	1.62	1.66	1.69	1.75	1.79
Glass Type	PSK2	SSK4 (SK16)	SSKN5	LaF23 (LAKN9)	LaFN2	LaF21
Year of Introduction	1890	1920	1930	1947	1952	1956

Monochromatic Fifth-Order Interpolating Aberrations

Designating g for Gaussian image size, $\bar{x}$ and $\bar{y}$ for ray co-ordinates in the entrance pupil, we introduce normalized co-ordinates:

$$H \equiv \frac{g}{g_{max}} \qquad p \equiv \frac{\bar{x}}{\bar{x}_{max}} \qquad q \equiv \frac{\bar{y}}{\bar{y}_{max}}$$

In these co-ordinates, the aberrations up to the fifth order for the meridional and main sagittal section are given in equations 3 and 4. The equations are arranged to give an immediate impression of their effect in terms of basic aberrations. The a_{ijk} are aberrations for H, p, q = 1 rather than aberration co-efficients.

		Spherical Aberration		Asymmetry Errors		Focal Surfaces		Distortion	
(3)	$\Delta y' =$	$a_{003}q^3$	$+ a_{102}Hq^2$		$+ a_{201}H^2q$		$+ a_{300}H^3$		Meridional Section
		$+ a_{005}q^5$	$+ a_{104}Hq^4$		$+ a_{401}H^4q$		$+ a_{500}H^5$		
		$+ a_{203}H^2q^3$	$+ a_{302}H^3q^2$						
(4a)	$\Delta x' =$	$a_{030}p^3$			$+ a_{210}H^2p$				Main Sagittal Section
		$+ a_{050}p^5$			$+ a_{410}H^4p$				
		$+ a_{230}H^2p^3$							
(4b)	$\Delta y' =$		$a_{120}Hp^2$				$+ a_{300}H^3$		
			$+ a_{140}Hp^4$				$+ a_{500}H^5$		
			$+ a_{320}H^3p^2$						

$$a_{030} = a_{003} \qquad 3a_{120} = a_{102}$$

$$a_{050} = a_{005} \qquad 5a_{140} = a_{104}$$

As all aberrations of third and fifth order are represented in the meridional and main sagittal section, full correction over the entire pupil within the validity of the fifth order can be obtained without additional information.

However, the numerical accuracy of this approximation is insufficient for the lenses under consideration if the conventional calculations from two first order ray traces are applied. To extend the usefulness of the fifth order model, we will, in the following, consider all a_{ijk} as derived from real ray traces, hopefully to combine simple structure and adequate accuracy. In [2] the increase in accuracy is discussed with regard to spherical aberration.

Considerations Regarding Correction

With constant glasses the basic Double Gauss lens (see Figure 2) provides 20 degrees of freedom: 10 radii, 6 thicknesses, 4 air spaces. This number is further reduced if we consider the following:

1. The thicknesses of the outer lenses and the adjacent spaces are to be fixed to minimum values required for manufacture.

2. If crown and flint component of the menisci have equal refractive index for the main wavelength, the cemented surfaces have no effect on monochromatic correction.

3. In order to strike a suitable compromise between lens diameter and vignetting, a maximum length between the outer vertices must not be exceeded, limiting the range of variation for thicknesses and spaces.

Thus we have 8 radii with full range variation, 2 thicknesses and 2 air spaces with restricted ranges of variation available for correction of 14 monochromatic aberrations.

The main application of the Double Gauss type is in "standard" lenses for the 35 mm format. Therefore, all lenses considered in the following will have a focal length of 52 mm and a speed of f/2.

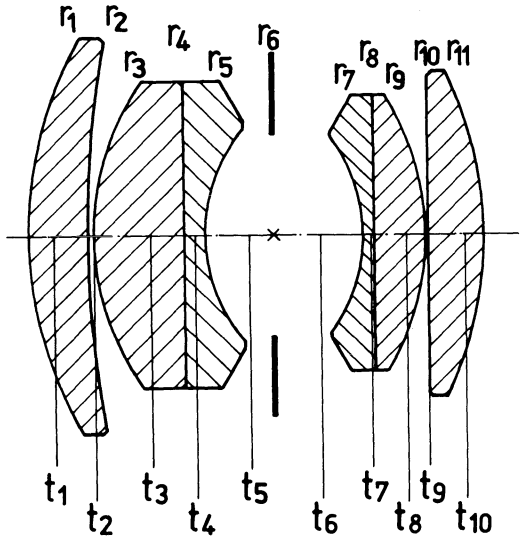

Figure 2. Double Gauss Lens

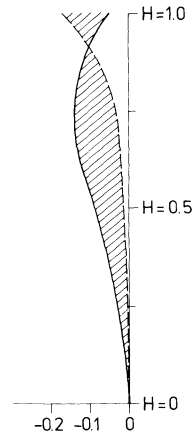

Figure 3. Astigmatic Field Curves

At full aperture the lens shall produce an image of a distant object on the film surface which is assumed to be plane and normal to the optical axis. The best focus for all parts of the field shall be the same and its variation with reducing aperture shall be moderate. The distortion shall be small enough as not to be obvious when critical objects (e.g. - architecture filling the entire format) are photographed.

Experience and theoretical considerations show that the oblique spherical aberrations are the most stubborn image errors of the Double Gauss lens and its variations. (Our aberrations a_{230} and a_{203}.) Furthermore, the sagittal field surface represented by a_{210} and a_{410} is very difficult to change, as a forced improvement is paid for by an increased zonal spherical aberration. The effect of residual field curvature can be moderated by introducing undercorrection that moves the best focus for the on-axis image closer to the lens than the Gaussian focal plane. However, the extent of this measure is limited by the ensuing change of focus with aperture. Correction of distortion is always aesthetically adequate if it does not exceed 1.5% at the corner of the frame. The best compromise for residual astigmatism is obtained by minimizing the area weighted absolute astigmatism (see Figure 3). In [2] this has been shown to require correction of astigmatism for H = 0.9.

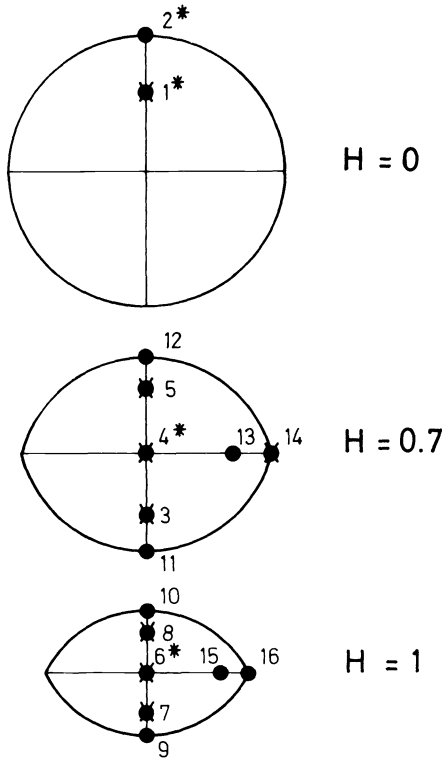

Figure 4.
Ray Distribution for SCIP

Application of the SCIP Programme

SCIP is an optical design package for small computers developed and marketed by Scientific Calculations Inc., Fairport, New York. Its optimization section is a Damped Least Squares programme that operates on first and third order and selected real ray aberrations. The theoretical background of ths DLS programme is described in [4,5] and details concerning the operation are given in [6]. The real rays available for optimization are shown in Figure 4. Asterisks indicate that differential rays along the marked rays are also being traced. The rays marked X will be used in the following calculations. Their respective co-ordinates in the entrance pupil and the definitions of the SCIP aberrations for these rays are given in Tables 3 and 4.

Table 3.

#	H	p/v	q/v
1*	0	0	0.7
3	0.7	0	0.7
4*	0.7	0	0
5	0.7	0	0.7
6*	1.0	0	0
7	1.0	0	-0.7
8	1.0	0	0.7
14	0.7	1.0	0

v indicates the vignetting. Different values may be given for maximum and zonal image size and for the respective meridional and main sagittal sections.

Table 4.

$TAZ \equiv \Delta y'_1$

$AZZ \equiv 0.5(y'_3 + y'_5) - y'_4$

$TFCM \equiv \frac{\partial}{\partial a}(y'_6)$

$SFCM \equiv \frac{\partial}{\partial p}(y'_6)$

$PACZ \equiv \frac{\partial}{\partial \lambda}(\Delta y'_1)\Delta\lambda$

$PLCM \equiv \frac{\partial}{\partial \lambda}(y'_6)\ \Delta\lambda$

$COMAZ \equiv \frac{\partial}{\partial H}\Delta y'_1$

$AEZ \equiv 0.5(y'_7 + y'_8) - y'_6$

$SZZ \equiv 0.5(y'_5 - y'_3)$

$XZM \equiv \Delta x'_{14}$

$DISTM \equiv y'_6 - g_{max}$

The monochromatic aberrations from the above table can be expressed in terms of the aberrations a_{ijk} up to the fifth order by inserting the appropriate values for H, p, q and v according to Table 3. Choosing meridional vignetting factors of 0.5 for H = 1 and 0.7 for H = 0.7 we obtain:

$TAZ \equiv 0.354\ a_{003} + 0.177\ a_{005}$

$COMAZ \equiv 0.5\ a_{102} + 0.25\ a_{104}$

$AZZ \equiv 0.226\ a_{102} + 0.072\ a_{104} + 0.113\ a_{302}$

$AEZ \equiv 0.181\ a_{102} + 0.032\ a_{104} + 0.181\ a_{302}$

$TFCM \equiv a_{201} + a_{401}$

$SFCM \equiv a_{210} + a_{410}$

$SZZ \equiv 0.28\ a_{201} + 0.14\ a_{401} + 0.181\ a_{003} + 0.058\ a_{005} + 0.09\ a_{203}$

$XZM \equiv 0.5\ a_{210} + 0.25\ a_{410} + a_{003} + a_{005} + 0.5\ a_{230}$

$DISTM \equiv a_{300} + a_{500}$

All a_{ijk} with the exception of a_{320} are represented. The missing aberration is a contribution to sagittal coma which is not available because only $\Delta x'$ and not $\Delta y'$ derived from rays 13, 14, 15 and 16 are being used by the programme. In [2] detailed considerations are given for the choice of aberrations, their target values, the use of the "correct" and "minimize" mode and the weights for the aberrations to be minimized. The following set of aberrations, targets and weights has been derived and used for all examples presented later.

Table 5. Set of Aberrations for Optimization.

Correct	Target	Minimize	Target	Weight
TAZ	-0.025	COMAZ	0	2
AZZ	0	AEZ	0	1
TFCM	-0.03	SZZ	-0.025	1
SFCM	-0.03	XZM	0	1
PACZ	0	DISTM	0	0.1
PLCE	0	VL	36	0.02
GSHT	-18.9			

Design Examples

The starting data for all examples are taken from Table 1. All lenses have a focal length of 52 mm, a maximum image size of 21 mm corresponding to a format of 24 x 36 mm^2, an aperture of f/2, and are corrected for an object at infinity.

In order to correct the 2 chromatic aberrations contained in the set given in Table 3, the menisci are split in 2 parts by a plano cementing surface. The resulting negative lenses are given a thickness of 1.3 mm, and the remaining thickness of the positive part is allowed to vary during optimization. The flint glasses are selected that their Abbe-value is approximately 2/3 of the Abbe-value of the attached crown lenses. Initially, the difference for the refractive indices of the main wavelength (λ=546 nm) is held close to zero. Later, the effect of index differences on the cemented surfaces is to be considered.

To facilitate the identification of different examples, a number code is assigned to the refractive indices listed in Table 1:

Refractive Index	1.57	1.62	1.66	1.69	1.75	1.79
Number Code	1	2	3	4	5	6

The number code serves as an abbreviated description of the materials used, e.g. 5225 is a lens whose outer elements are made of glass with n = 1.75, and the inner menisci of glass with n = 1.62. By adding the number of iterations required for convergence of the optimization, we can also indicate the efficiency of the programme for a particular lens, e.g. 5225/7 means that, in this case, 7 iterations were needed.

The state of correction is shown by plots of lateral aberrations over normalized entrance pupil co-ordinates in the meridional and main sagittal sections for image sizes of 0, 10.5, 15.75, and 21 mm. To avoid crowding, only $\Delta x'$ is plotted for the main sagittal section. The amount of sagittal coma for p=1, y'=15.75 is given below the graph. This type of plot does not show distortion, which is, therefore, also given below the graph for y'=21. Colour correction to show $\Delta y'$ has been plotted for 3 colours for y'=0 and y'=15.75.

———————————— $\Delta y'$ for "e" (λ = 546 nm)

— — — — — — — — — — — — — — $\Delta x'$ for "e"

——— · ——— · ——— · ——— $\Delta y'$ for "C" (λ = 656 nm)

— · — · — · — · — · — · — · — $\Delta y'$ for "g" (λ = 436 nm)

Vignetting is being considered by plotting in the meridional section only to q = .5 for y' = 21, to q = .67 for y' = 15.75 and to q = .83 for y' = 10.5. However, aberrations larger than 75μ are omitted from plotting to keep the graphs clear. Therefore, one has to consider additional image deterioration whenever the aberration curves are shorter than indicated above.

Figures 5 and 6 show the improvement of lens 4444 in 5 iterations of the optimization programme. There are only monochromatic aberrations plotted because the graph for the starting configuration 4444/0 is 20 times coarser than all others, and chromatic aberrations could not be distinguished.

Lenses 1111/6 through 6666/11 (Figures 7, 8, 11, 12, 13, 15 - data given in Table 6) demonstrate the change in correction potential with increasing refractive indices. The zones of astigmatism and the oblique spherical aberrations become smaller. However, the sagittal field curvature increases. This observation can be useful when designing for smaller aperture. Distortion for all 6 examples is smaller than 1%, and the amount of sagittal coma remains below 0.03. The latter confirms that the omission of an aberration containing a_{320} from the optimization routine of SCIP has not seriously effected the correction.

Lens 2222/6 can be compared to examples L1[3] (Figure 9) and L2[4] (Figure 10). L1 is taken from Lee's original "Optic" patent. Lens 2222/6 demonstrates that no index difference on the cemented surfaces is required. L2 is the most recent basic Double Gauss lens without index differences at the cemented surfaces that could be found. It favours contrast, which results in a larger variation of coma over the field and in an increased shift of focus with aperture.

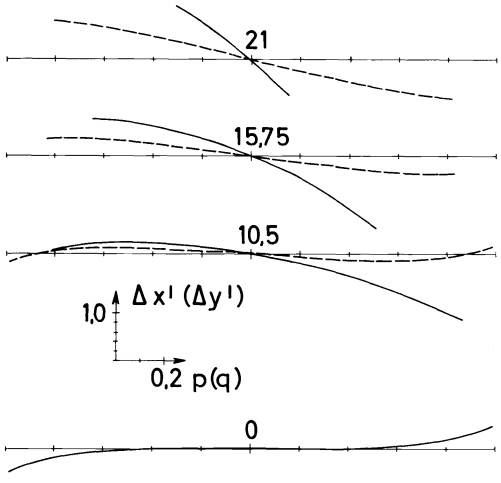

Figure 5. Lens 4444/0 (e only)

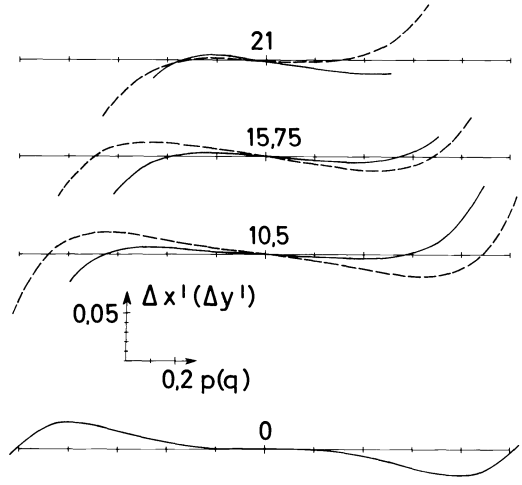

Figure 6. Lens 4444/5 (e only)

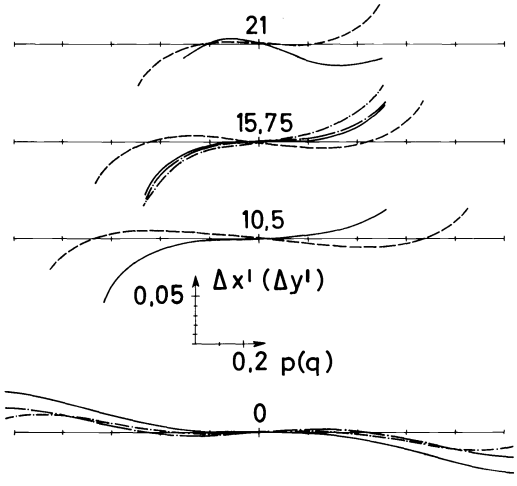

Figure 7. Lens 1111/6
Dist. 0.00% Sag. Coma -0.002

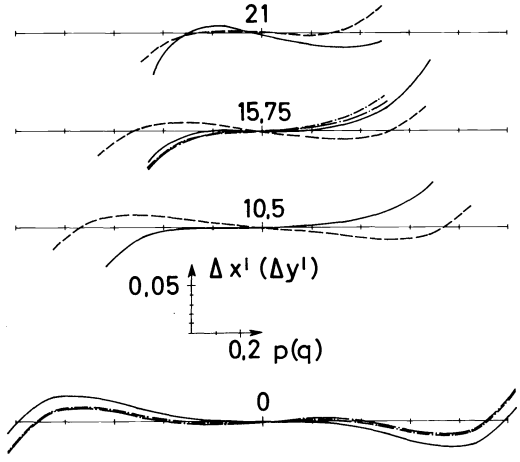

Figure 8. Lens 2222/6
Dist. 0.25% Sag. Coma -0.002

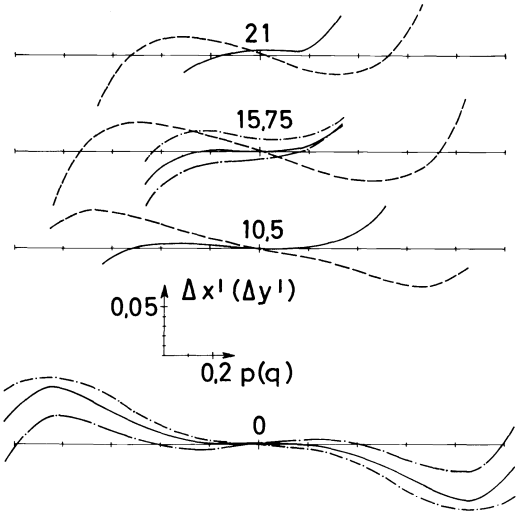

Figure 9. Lens L1 (Lee)
Dist. 0.42% Sag. Coma 0.145

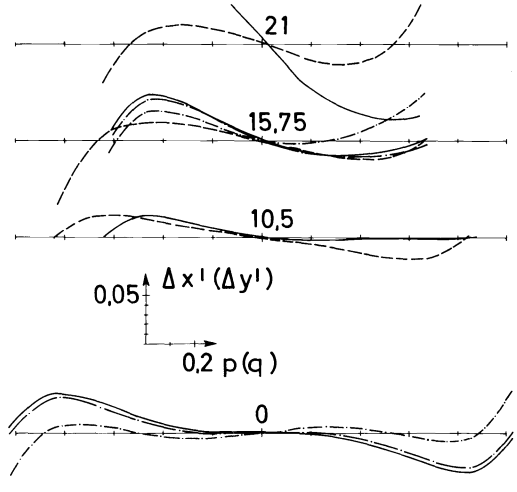

Figure 10. Lens L2 (Baker)
Dist. -0.18% Sag. Coma -0.033

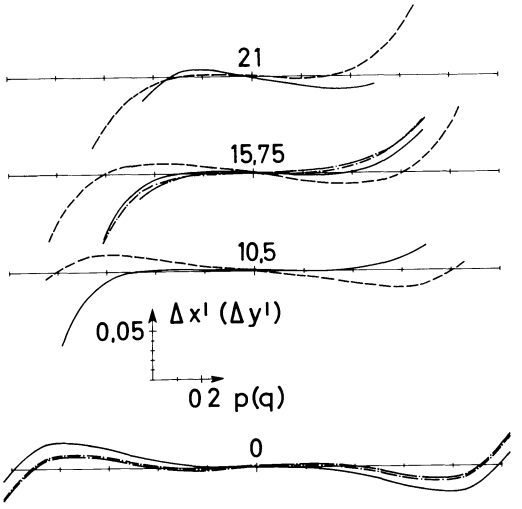

Figure 11. Lens 3333/5
Dist. -0.13% Sag. Coma 0.011

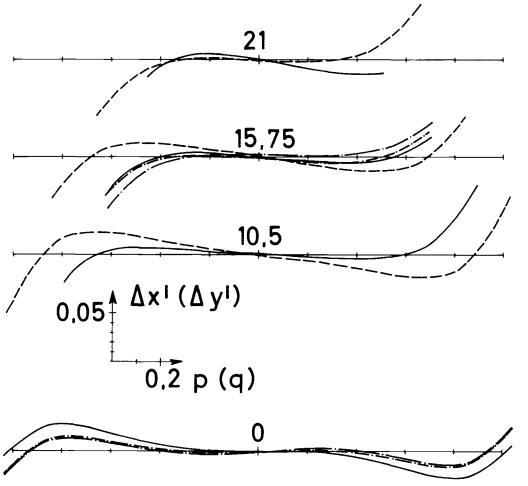

Figure 12. Lens 4444/5
Dist. -0.43% Sag. Coma 0.021

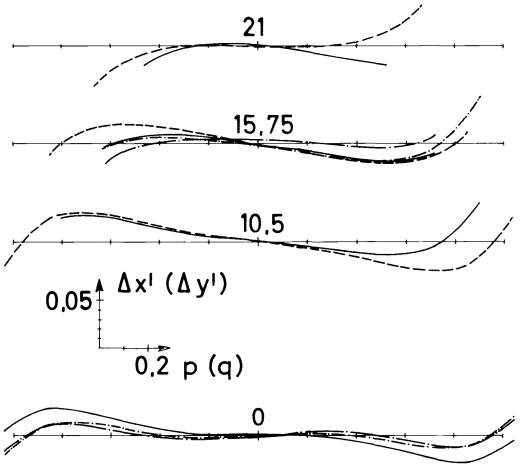

Figure 13. Lens 5555/5
Dist. -0.52% Sag. Coma 0.027

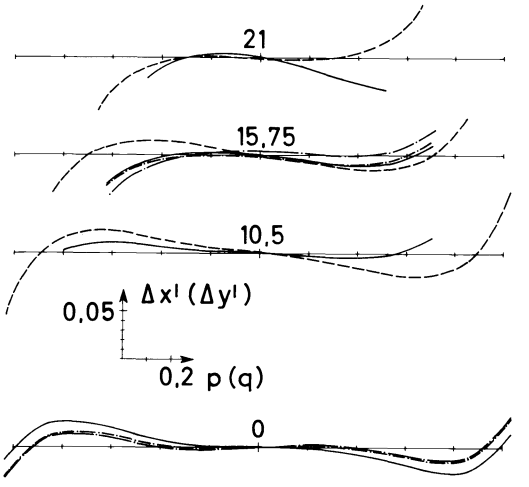

Figure 14. Lens 2444/5
Dist. -0.47% Sag. Coma 0.035

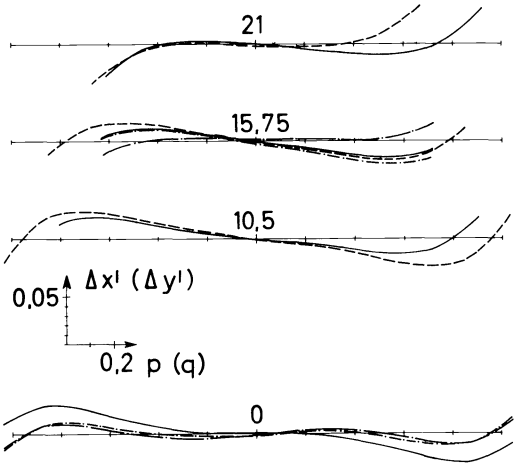

Figure 15. Lens 6666/11
Dist. -1.00% Sag. Coma 0.022

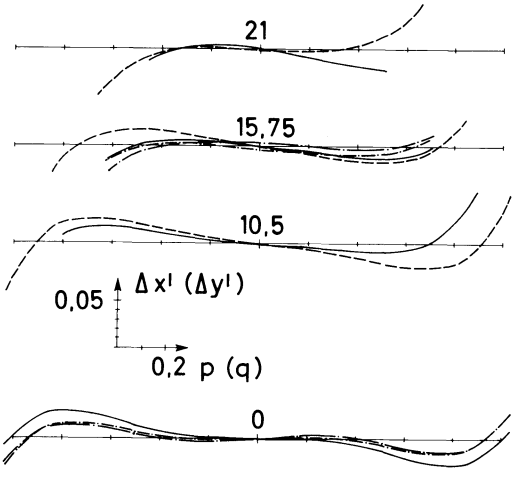

Figure 16. Lens 4445/4
Dist. -0.30% Sag. Coma 0.027

Table 6. Lens Data

Surf. #	1	2	3	4	5	6	7	8	9	10	11
1111/6											
r	27.76	113.73	18.50	-133.06	11.37	Stop	-13.08	-189.65	-16.32	96.98	-45.27
t	4.00	0.20	7.40	1.30	6.27	5.68	1.30	6.36	0.20	4.00	32.09
	PSK 2	Air	PSK 2	LF 6	Air	Air	LF 6	PSK 2	Air	PSK 2	Air
2222/6											
r	28.21	101.31	19.11	468.51	11.91	Stop	-13.52	-259.82	-17.76	190.75	-35.26
t	4.00	0.20	7.15	1.30	5.90	6.59	1.30	5.79	0.20	4.00	32.19
	SSK 4	Air	SSK 4	F 2	Air	Air	F 2	SSK 4	Air	SSK 4	Air
3333/5											
r	29.56	95.08	19.70	142.19	12.51	Stop	-14.17	-115.47	-19.01	198.46	-35.74
t	4.00	0.20	7.25	1.30	5.82	6.82	1.30	5.46	0.20	4.00	31.90
	SSK N5	Air	SSK N5	SF 51	Air	Air	SF 51	SSK N5	Air	SSK N5	Air
4444/5											
r	30.92	92.93	20.14	93.66	13.00	Stop	-14.81	-72.11	-20.12	175.02	-37.76
t	4.00	0.20	7.47	1.30	5.75	6.87	1.30	5.28	0.20	4.00	31.32
	LaF 23		LaF 23	SF 8			SF 8	LaF 23		LaF 23	
5555/5											
r	33.73	91.73	20.55	71.16	13.75	Stop	-15.95	-52.21	-21.52	146.90	-44.07
t	4.00	0.20	7.64	1.30	5.80	6.92	1.30	5.00	0.20	4.00	30.51
	LaF N2		LaF N2	SF 13			SF 13	LaF N2		LaF N2	
6666/11											
r	36.03	90.71	20.07	29.61	13.98	Stop	-16.35	-36.17	-21.36	156.69	-49.57
t	4.00	0.20	6.81	1.30	7.02	6.84	1.30	5.12	0.20	4.00	31.70
	LaF 21		LaF 21	SF 11			SF 11	LaF 21		LaF 21	

Lens 6666/11 is the best corrected one monochromatically. However, the colours at 3/4 field are fanning. This occurs because there was no flint glass with good chemical stability available that gave the recommended ratio of Abbe-values of approximately 2/3.

In [2] the effect of different combinations of refractive indices (while maintaining zero difference at the cemented surfaces) has been investigated. The main conclusion is that lowering the index of the first lens gives the smallest decrease, and raising it in the last lens, the biggest improvement in overall correction. The respective examples 2444/5 and 4445/6 are shown in Figures 14 and 16. These findings are useful for reducing the cost of materials while maintaining or improving image quality.

Finally, we will briefly address the question concerning the effects that the introduction of differences in main refractive index at the cemented surfaces will produce. When doing so within the group of 6 indices used, so far no improvement could be obtained. On the contrary, the state of correction deteriorated, particularly regarding the meridional coma for larger apertures whose variation across the field became more pronounced. As the set of aberrations for optimization had been the same as previously described, the introduction of other and/or additional aberrations, targets and weights more suited to the additional degrees of freedom might have lead to a more effective optimization. However, this would have been outside the scope of a single design procedure in its narrowest sense. Therefore, the limitation to only 6 refractive indices was given up in order to try the results of smaller index differences at the cemented surfaces.

By choosing suitable small differences, the meridional coma at half-field could be improved. Differences in the front meniscus proved to be the most effective ones. (It is important to remember that all optimization runs for these examples started from data taken or interpolated from Table 1, rather than from corrected lenses.)

Lens 3 5SF1 5 6 (Figure 17) and Lens 3 5SF1 1.72 6 (Figure 18) are given as examples. Lens 3 5SF1 1.72 6 is considered to be the cost-performance optimum resulting from this study. The corresponding data can be found in Table 7 and Table 8.

Table 7. Lens Data

Surf. #	1	2	3	4	5	6	7	8	9	10	11
4 5-SF1 5 6 /5											
r	33.54	95.63	19.93	85.84	13.54	Stop	-16.10	-49.74	-21.98	185.72	-45.52
t	4.00	0.20	7.19	1.30	5.92	6.91	1.30	5.23	0.20	4.00	31.02
	LaF 23	Air	LaF N2	SF 1	Air	Air	SF 13	LaF N2	Air	LaF 21	Air

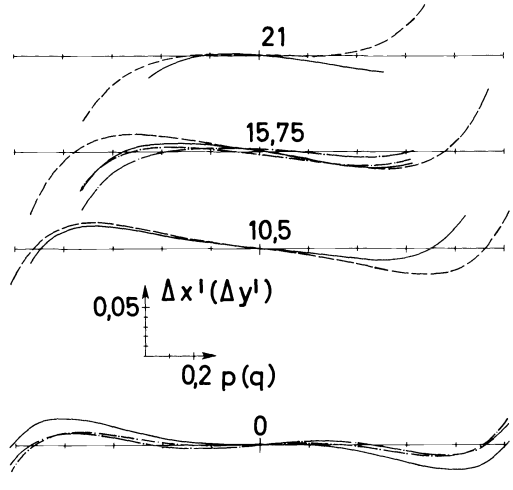

Figure 17. Lens 4 5-1.72 5 6/5
Dist. -0.56% Sag. Coma 0.028

Table 8. Lens Data

Surf. #	1	2	3	4	5	6	7	8	9	10	11
4 5-SF1 1.72 6 /5											
r	33.10	94.15	20.71	92.11	13.52	Stop	-15.92	-60.22	-21.82	203.62	-43.85
t	4.00	0.20	7.23	1.30	5.91	6.89	1.30	5.23	0.20	4.00	31.04
	LaF 23	Air	LaF N2	SF 1	Air	Air	SF 1	LaF N3	Air	LaF 21	Air

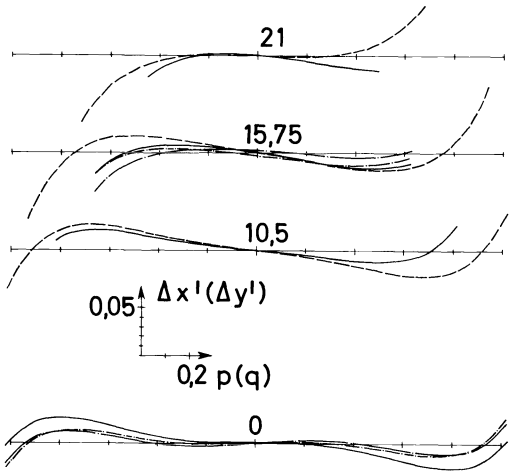

Figure 18. Lens 4 5-1.72 1.72 6/5
Dist. -0.50% Sag. Coma 0.0028

Conclusion

For smaller optimization programmes, the use of sets of aberrations closely related to image error theory can significantly increase the effectiveness.

References

1. Y. Matsui, H. Hirose, Some Experiments on Automatic Optical Design, Japan J. Applied Phys. 4 Suppl. 1 (1965) p. 86-92.
2. W. Mandler, Über Die Berechnung Einfacher Gauss-Objektive, "Optik", Vol. 55, 1980 p. 119-140 and 219-240.(Thesis Justus-Liebig-Universität Gießen 1979, Fachbereich Physik)
3. DRP 92313, 1895, Astigmatisch, sphaerisch und chromatisch korrigiertes Objektiv. Inv. P. Rudolph, assigned to Fa. Carl Zeiss.
4. G.H. Spencer, A Flexible Automatic Lens Correction Procedure, Appl. Optics, Vol. 2 (1963) p. 1257-1264.
5. G.H. Spencer, A Computer Oriented Automatic Lens Correction Procedure, (Thesis, University of Rochester, Rochester, N.Y., 1963).
6. SCIP Optical Design Program (Manual), Scientific Calculations Inc., Fairport, New York.
7. Brit. Patent 157.040, 1920, Improvements in Lenses for Photography and the like, Inv. H.W. Lee, assigned to Taylor, Taylor & Hobson.
8. U.S. Patent 1.532.751, 1950, Highly Corrected Objektive having Two Inner Divergent Meniscus Components between Collective Components, Inv. J.G. Baker, assigned to Perkin-Elmer Corporation.